

Effect of concentrated masses with rotary inertia on vibrations of rectangular plates

M. Amabili^{*,1}, M. Pellegrini, F. Righi, F. Vinci

Dipartimento di Ingegneria Industriale, Università di Parma, Parco Area delle Scienze 181/A, Parma, I-43100 Italy

Received 28 October 2004; received in revised form 27 October 2005; accepted 14 November 2005

Available online 11 April 2006

Abstract

The effect of attached masses on free vibrations of rectangular plates is studied by considering rotary inertia of concentrated masses and geometric imperfections of the plate. Experiments are performed to understand the changes in natural frequencies and mode shapes. In order to validate and better understand the experiments, numerical results are also presented. Boundary conditions at the plate edges are those of simply supported plate with additional rotational springs at the plate edges. By tuning the stiffness of these springs, any boundary conditions comprised between simply supported and clamped edges can be simulated. Numerical results are successfully compared to experiments performed on a stainless-steel plate with an attached mass of different translational and rotary inertia. In particular, it is shown that a small mass placed on the diagonal of a square thin plate is enough to transform the shape of modes with one nodal line parallel to the edge, into diagonal modes, i.e. modes with diagonal nodal lines. Rotary inertia of concentrated masses reduces significantly natural frequencies. Moreover, additional modes due to the presence of large rotary inertia of concentrated masses arise, which do not appear if rotary inertia is neglected. Finally it is shown that masses placed only on one side of the plate or symmetrically (with respect to the mid-plane) placed on both sides give similar results.

© 2006 Elsevier Ltd. All rights reserved.

1. Introduction

Vibrations of rectangular plates carrying concentrated masses have interested researchers since the beginning of the last century, as testified by the paper of Gershgorin [1] published in 1933. Since that time many studies have been published. Some of the earlier studies were reviewed in Leissa's monograph [2]. No rotary inertia of the attached masses was considered in these studies; the addition of this effect can be found in Refs. [3–6]. In particular, Stokey and Zorowski [3] considered rotary inertia of attached masses; the solution was obtained by roots of approximate equations. Geometric imperfections of the plate were not considered. Numerical results were compared to experiments, but only the fundamental mode of vibration of rectangular plates with one or two masses attached were investigated; therefore, no additional modes due to rotary inertia of masses (i.e. modes that do not appear if rotary inertia of masses is neglected) were identified. Shah and

^{*}Corresponding author. Tel.: +39 0521 905896; fax: +39 0521 905705.

E-mail address: marco.amabili@unipr.it (M. Amabili).

¹<http://me.unipr.it/mam/amabili/amabili.html>

Datta [4] developed an alternative method to find approximate natural frequencies of rectangular plates simply supported (or with mixed boundary conditions simply supported/clamped) carrying concentrated masses with rotary inertia. The first three natural frequencies are reported for a square plate carrying one mass at different positions, but no investigation of mode shapes is reported (some evident printing errors appear in the numerical results).

Nicholson and Bergman [5] studied vibration of thick, simply supported plates carrying concentrated masses and retained effects of transverse shear and rotary inertia of each mass. Transverse shear and rotary inertia of the thick plate was considered by using Mindlin's plate theory, but the limit case of thin plate was also investigated. Only one numerical case was studied for a square plate with a central mass having center of mass on the plate surface, i.e. with small rotary inertia, becoming almost zero for the limit case of thin plate.

More recently Singal and Gorman [6] compared analytical and experimental results for rectangular aluminum plates on rigid point supports and carrying one central mass or two masses of different weights. Analytical solution was obtained by introducing in the equations of motion of the plate a dynamic force to take into account translation inertia and two dynamic couples (two pairs of opposing forces) to take into account rotary inertia for each mass. Results show that rotary inertia reduces natural frequencies (e.g. 8% in one of the studied cases with central mass). No additional modes due to rotary inertia of masses were detected. This is probably due to the relatively small rotary inertia of the masses used in calculations and experiments with respect to their weight.

Rotary inertia of attached masses was considered in the paper of Laura et al. [7] on vibrations of beams and plates supported at the edges and elastically restrained against rotation. Solution was obtained by using the Rayleigh–Ritz method. Results are presented only for the fundamental mode and show a significant reduction of the natural frequency due to rotary inertia. Awrejcewicz and Krysko [8,9] considered the effect of rotary inertia of concentrated masses by using a 3-D theory to model the plate. The effect of rotary inertia of concentrated masses has not been numerically studied.

Additional recent studies [10–12] on the effect of concentrated masses consider additional complications or different geometries but do not include the effect of rotary inertia.

In the present study, the effect of concentrated masses on free vibrations of rectangular plates is investigated by considering rotary inertia of concentrated masses and geometric imperfections of the plate. The study is driven by experiments, and the numerical results, obtained by using a self-developed Rayleigh–Ritz computer program, are used to validate and better understand the experiments. Results show that: (i) a small mass placed on the diagonal of a square thin plate is enough to transform the shape of modes ($m = 1, n = 2$) and ($m = 2, n = 1$), where m and n are the numbers of half-waves in the two orthogonal directions in the plate plane, into diagonal modes, i.e. modes with diagonal nodal lines; (ii) large rotary inertia of concentrated masses introduces additional modes, which do not appear if rotary inertia is neglected; (iii) masses placed only on one side of the plate or symmetrically (with respect to the mid-plane) placed on both sides give similar results; and (iv) geometric imperfections can play a significant role. Points (i–iv) are important to better understand the physics of the plate with added masses. They have practical applications; e.g. point (iii) indicates that in a FEM model it is sufficient to model added masses with large rotary inertia with lumped elements and it is not necessary to use 3-D elements.

2. Theoretical approach

A rectangular plate with coordinate system (O; x, y, z), having the origin O at one corner is considered (see Fig. 1). The displacements of an arbitrary point of coordinates (x, y) on the middle surface of the plate are denoted by u, v and w , in the x, y and out-of-plane (z) directions, respectively. Initial geometric imperfections of the rectangular plate associated with zero initial tension are denoted by out-of-plane displacement w_0 ; only out-of-plane initial imperfections are considered.

The boundary conditions are those of a simply supported plate with movable edges in the x – y plane; distributed rotational springs are placed at four boundaries. In order to reduce the system to finite dimensions, the middle surface displacements u, v and w are expanded by using approximate functions, which satisfy

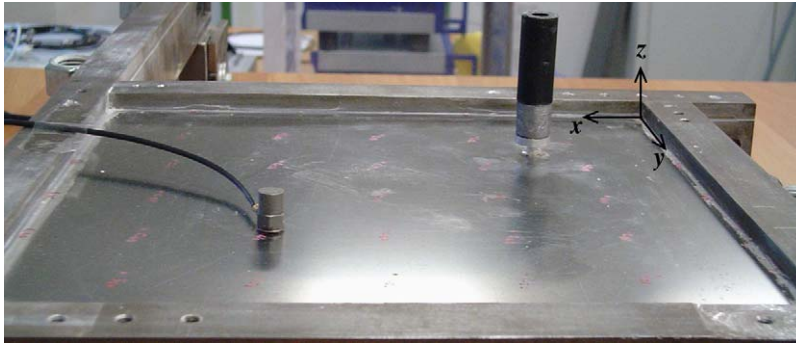


Fig. 1. Photograph of the plate with two attached masses on both sides and accelerometer: Case 2. The coordinate system is shown.

identically the geometric boundary conditions:

$$u(x, y, t) = \sum_{m=1}^M \sum_{n=1}^N u_{m,n}(t) \cos(m\pi x/a) \sin(n\pi y/b), \quad (1)$$

$$v(x, y, t) = \sum_{m=1}^M \sum_{n=1}^N v_{m,n}(t) \sin(m\pi x/a) \cos(n\pi y/b), \quad (2)$$

$$w(x, y, t) = \sum_{m=1}^M \sum_{n=1}^N w_{m,n}(t) \sin(m\pi x/a) \sin(n\pi y/b), \quad (3)$$

where m and n are the numbers of half-waves in x and y directions, respectively, and t is the time; $u_{m,n}(t)$, $v_{m,n}(t)$ and $w_{m,n}(t)$ are the generalized coordinates that are unknown (harmonic functions of t in case of free vibrations). M and N indicate the number of terms necessary in the expansion to reach convergence of the solution.

The imperfection w_0 is expanded as

$$w_0(x, y) = \sum_{m=1}^{\tilde{M}} \sum_{n=1}^{\tilde{N}} A_{m,n} \sin(m\pi x/a) \sin(n\pi y/b), \quad (4)$$

where $A_{m,n}$ are the modal amplitudes of imperfections; \tilde{N} and \tilde{M} are integers indicating the number of terms in the expansion.

The solution is obtained by an eigenvalue problem for symmetric matrices of dimension $(3M \times N) \times (3M \times N)$ by using a standard Rayleigh–Ritz procedure, see Ref. [13] for details.

3. Experimental and numerical results

3.1. Comparison with available results

A comparison with theoretical and experimental results published by Stokey and Zorowski [3] has been performed in order to validate the numerical model developed. Calculations have been performed for a simply supported aluminium plate, with movable edges in the x – y plane, having the following dimensions and material properties carrying a single mass as specified in Table 1: $a = b = 0.508$ m, $h = 0.00231$ m, $E = 70 \times 10^9$ Pa, $\rho = 2749$ kg/m³ and $\nu = 0.33$. Present results have been obtained by using $N = M = 10$ in the Rayleigh–Ritz expansion. Considering the approximation of numerical and experimental results reported in Ref. [3], the comparison is very reasonable.

3.2. Experimental and numerical results for a plate with a mass on the diagonal

Experiments in laboratory have been conducted on an almost square stainless-steel plate with the following dimensions and material properties: $a = 0.210$ m, $b = 0.2085$ m, $h = 0.0003$ m, $E = 198 \times 10^9$ Pa, $\rho = 7850$ kg/m³ and $\nu = 0.3$. The plate was inserted into a heavy rectangular steel frame made of a few thick parts, see Fig. 1, having grooves designed to hold the plate. Silicon was placed into the grooves to hold better the edges of the plate and then avoid out-of-plane displacements at the edges. The in-plane displacements at the edges, in direction orthogonal to the edge itself, were allowed because the constraint given by silicon on this displacement was small. The in-plane displacements parallel to the edges were restrained by friction between the panel and the grooves and by silicon. Therefore the experimental boundary conditions are close to those of a simply supported plate with movable edges in the x - y plane.

The plate has been subjected to impact excitation in order to identify the natural frequencies and modes shapes by experimental modal analysis. The panel response has been measured on a grid of 50 points, the excitation has been provided by a miniature instrumented hammer *B&K* 8203. The plate response has been measured by using a Polytec laser Doppler vibrometer (sensor head OFV-505 and controller OFV-5000). The time responses have been measured by using the Difa Scadas II front-end connected to a HP c3000 workstation and the software CADA-X of LMS for signal processing and data analysis. Frequency Response Functions (FRFs) have been estimated by using averages of 8 measurements and H_V algorithm.

Table 2 shows a comparison among experimental and theoretical natural frequencies of the plate (first nine modes, identified by using number of half-waves in x and y directions). In the numerical simulations both (i) rotational stiffness $k = 0$ and (ii) $k = 4.5$ N/rad have been used to simulate the effect of silicon; the introduction of these springs change only a little the frequencies, making them closer to experimental results. However, these differences for $k = 0$ with respect to experimental results can also be attributed to geometric imperfections of the plate, as it is discussed in Section 3.4.

Then, a mass of 0.0112 kg with rotary inertia $J_x = J_y = 0.205 \times 10^{-5}$ kg m² has been placed at $x_1 = a/4$ and $y_1 = b/4$, i.e. on the diagonal of the plate, mid-way between the corner and the centre. Theoretical and

Table 1
Comparison of present results and Ref. [3]

Mass (kg)	Rotary inertia (kg m ²)	Position	Experiments, Ref. [3]; (Hz)	Theory, from Ref. [3]; (Hz)	Present results (Hz)
0.91	0	$x_1 = a/2; y_1 = b/2$	23.4	23.5	22.9
5.4	0	$x_1 = a/2; y_1 = b/2$	11.0	11.0	10.6
1.34	2.37×10^{-3}	$x_1 = a/4; y_1 = b/2$	26.0	25.1	23.75
1.34	2.37×10^{-3}	$x_1 = a/4; y_1 = b/4$	28.5	28.7	27.3

Table 2
Natural frequencies of the plate

Mode (m, n)	Theoretical frequency (Hz); $k = 0$	Theoretical frequency (Hz); $k = 4.5$ N	Experimental frequency (Hz)
1, 1	32.7	38	38.1
1, 2	81.4	87.1	81.1
2, 1	82.1	88.0	91.4
2, 2	131	137	136
1, 3	163	169	165
3, 1	165	171	168
2, 3	212	218	212
3, 2	213	219	220
3, 3	294	300	296

Table 3

Natural frequencies of the plate with mass $I = 0.0112$ kg and $J_x = J_y = 0.205 \times 10^{-5}$ kg m²

Mode	Theoretical frequency (Hz)	Experimental frequency (Hz)
1	36.0	36.0
2	70.6	69.7
3	87.0	88.4
4	118	114
5	156	148
6	157	154
7	188	173

experimental natural frequencies are given in Table 3 and compare well each other. Mode shapes are compared in Table 4. Modes are no more identified by the number of half-waves because they are deformed by the presence of the mass. In particular, it is interesting to observe that the second and third mode are (1, 2) and (2, 1) for the plate without mass; they have one nodal line parallel to one of the edges; these modes become modes with one diagonal nodal line (diagonal modes) in presence of the attached mass as shown by modes 2 and 3 in Table 4. This is an interesting phenomenon that calculations show to appear already for a mass of a few grams for the studied plate. Therefore, an accelerometer placed on the plate can transform the original (1, 2) and (2, 1) modes into diagonal modes, affecting measurements. Therefore, for thin plates non-contact sensors should be preferred.

3.3. Experimental and numerical investigation on the effect of rotary inertia of a attached mass

The same plate studied in Section 3.2 is experimentally and numerically investigated here, but a PCB accelerometer (model M352C66) of 2 g placed at $x_2 = 0.75 \times a$, $y_2 = 0.75 \times b$ has been used to measure the plate response, and its mass and rotary inertia have been taken into account in the calculations. Two masses of 0.021 g have been placed symmetrically with respect to plane $z = 0$, both at $x_1 = a/4$, $y_1 = b/4$ on the two surfaces of the plate (see Fig. 2). Two different experimental configurations have been used in order to have very different rotary inertia of the masses, as shown in Figs. 1 and 2. In fact, these two masses are composed by a plastic hollow cylinder (very light) and a lead solid cylinder; switching the position of these two parts, an almost 4.5 times different rotary inertia can be obtained for the same mass. Table 5 summarizes these configurations, where also the ideal case with zero rotary inertia (Case 1) has been considered in numerical simulations. In numerical calculations $N = M = 18$ has been assumed to guarantee convergence of modes.

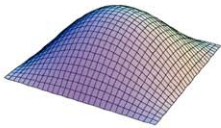
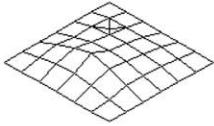
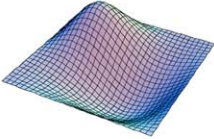
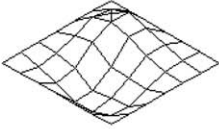
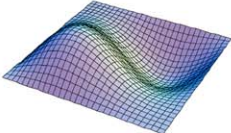
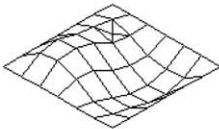
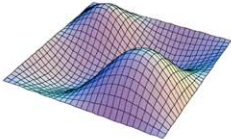
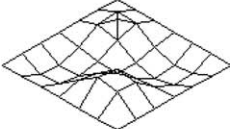
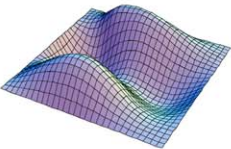
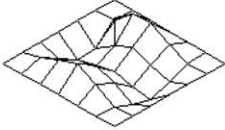
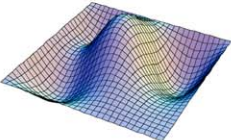
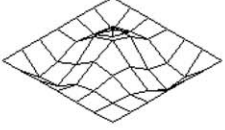
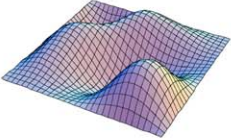

A comparison of computed natural frequencies of the first eight modes for the three different values of rotary inertia (Cases 1–3) is given in Table 6. Table 6 shows that the introduction of the rotary inertia from Cases 1 to 2, and then the increase of rotary inertia from Cases 2 to 3, gives a significant reduction of natural frequencies. But the most interesting phenomenon is that large rotary inertia give rise to two additional modes, in the studied frequency range, that are not obtained for the same mass neglecting rotary inertia (Case 1). These two additional modes are the 4th and 5th mode (modes F and G) in case of moderately large rotary inertia (Case 2), but become the 2nd and 3rd mode (modes B and C) in case of large rotary inertia (Case 3). These additional modes present a dominant displacement in the area of the large mass with significant rotation of the plate surface. The phenomenon of additional modes appearing as a consequence of large rotary inertia of attached masses probably has never been reported before.

Tables 7–9 compare experimental and computed natural frequencies and mode shapes for Cases 2 and 3, showing a very good agreement. Therefore the additional modes due to large rotary inertia are not only computational, but they are actual modes of the plate.

Finally a variant of Case 3 has also been experimentally studied placing the whole mass (actually 0.043 kg instead of 0.042 kg), with almost the same rotary inertia (actually 5.4×10^{-5} kg m² instead of 5.87×10^{-5} kg m²), on one side only of the plate at the same position $x_1 = a/4$, $y_1 = b/4$, i.e. making the system not symmetric with respect to the plane $z = 0$. Differences in frequency for the first mode is negligible,

Table 4

Mode shapes of the plate with mass $I = 0.0112$ kg and $J_x = J_y = 0.205 \times 10^{-5}$ kg m²

Mode	Theory	Experiment
1		
2		
3		
4		
5		
6		
7		

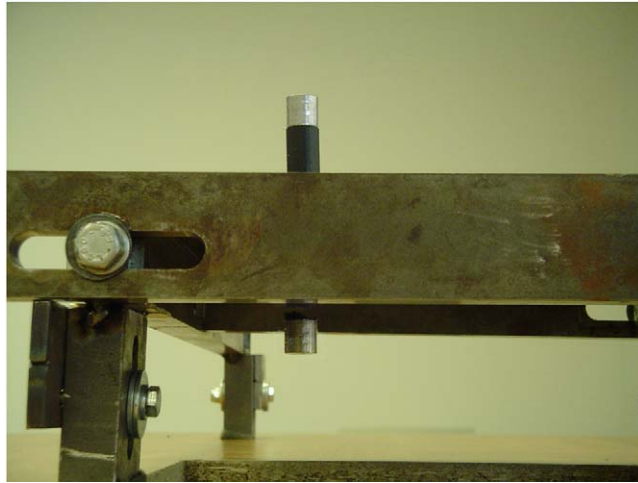


Fig. 2. Photograph of the plate with particular of the two attached masses: Case 3.

Table 5
Mass and rotary inertia for the three cases studied

	Mass (kg)	Rotary inertia (kg m^2)
Case 1	0.042	0
Case 2	0.042	1.32×10^{-5}
Case 3	0.042	5.87×10^{-5}

Table 6
Theoretical natural frequencies for the three cases studied

Mode	Frequency (Hz)		
	Case 1	Case 2	Case 3
A	25.7	25.2	23.1
B	—	—	37.7
C	—	—	42.1
D	49.5	49.3	50.2
E	81.8	68.7	84.4
F	—	73.1	—
G	—	87.3	—
H	102	107	106
I	153	158	158
L	164	172	172

as indicated by the sum of all the estimated FRFs shown in Fig. 3, except for modes B and C, which are the additional modes due to rotary inertia. For these modes a small shift on the left in frequency is shown, that cannot be attributed to the small change in the rotary inertia. Therefore the symmetry of the mass distribution with respect to plane $z = 0$ seems to have a small quantitative effect only on these additional modes B and C.

Table 7
Comparison of experimental and theoretical natural frequencies for Case 2

Mode	Theoretical frequency (Hz) Case 2	Experimental frequency (Hz) Case 2
A	25.2	25.4
B	—	—
C	—	—
D	49.3	53.0
E	68.7	61.6
F	73.1	66.2
G	87.3	88.2
H	107	105
I	158	152
L	172	170

Table 8
Comparison of experimental and theoretical natural frequencies for Case 3

Mode	Theoretical frequency (Hz) Case 3	Experimental frequency (Hz) Case 3
A	23.1	24.0
B	37.7	34.1
C	42.1	39.1
D	50.2	49.1
E	84.4	88.1
F	—	—
G	—	—
H	106	105
I	158	161
L	172	170

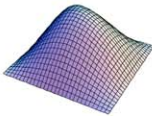
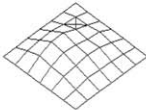
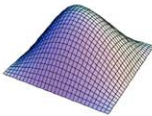
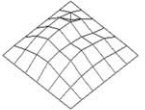
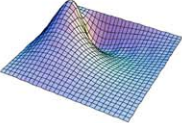
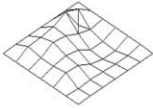
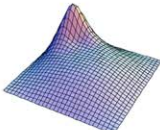
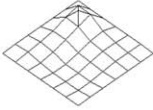
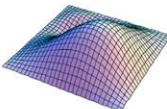
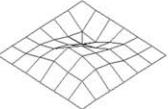
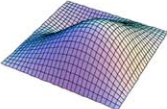
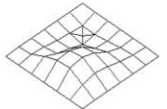
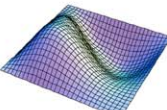

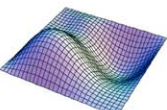

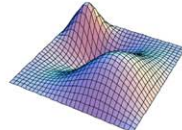
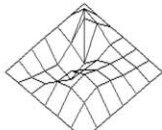
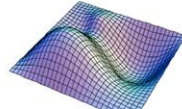
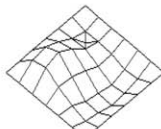
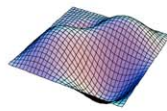
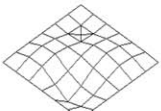
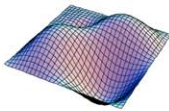
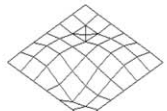
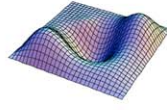
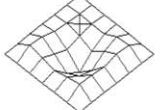
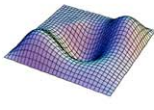
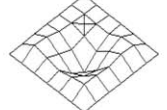
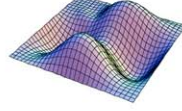
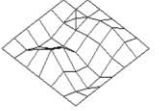
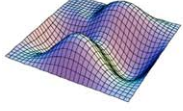
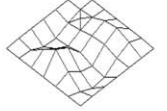
3.4. Measurement of geometric imperfections of the plate and their role on natural frequencies

Geometric imperfections of the plate used in the experiments have been measured by using a 3-D laser scanning system VI-910 Minolta. The contour plot indicating the deviation from the ideal flat surface is reported in Fig. 4. This figure shows that the actual shape of the plate is closer to a very shallow spherical shell; this is probably due to residual stresses of lamination in the steel foil. Geometric imperfections are always present in actual plates, and their introduction in the present study has practical interest.

Fig. 5 shows the computed natural frequency of the fundamental mode of the plate without masses versus the amplitude of geometric imperfections $A_{1,1}$, i.e. the imperfection that gives to the plate the shape of a spherical shallow shell. Simulations have been performed with $N = M = 5$. This deviation from flat surface makes the plate stiffer, and the natural frequency of the fundamental mode (1,1) is largely increased. The introduction of geometric imperfections (curvature) of the plate also couples in-plane and out-of-plane displacements in the equations of motion. The presence of imperfection can justify the differences in Table 2 among experiments and numerical results for $k = 0$. Actually Fig. 5 cannot be directly used to evaluate the frequency of the fundamental mode of the actual plate; in this case the deviation from the flat surface must be expanded in a double Fourier sine series, see Eq. (9), and then the global effect of imperfections must be evaluated with an expansion involving many modes in order to reach convergence of the solution.

The combined effects of added masses with rotary inertia and geometric imperfection $A_{1,1}$ is shown in Fig. 5 for the fundamental mode, obtained for the Case 3 investigated in Section 3.3 ($N = M = 5$ in the calculations). Comparison of Figs. 5 and 6 show that the effect of imperfections is reduced for the plate with

Table 9
Comparison of theoretical and experimental mode shapes for Cases 2 and 3

Mode	Case 2		Case 3	
	Theory	Experiment	Theory	Experiment
A				
B				
C				
D				
E				
F				
G				
H				
I				
L				

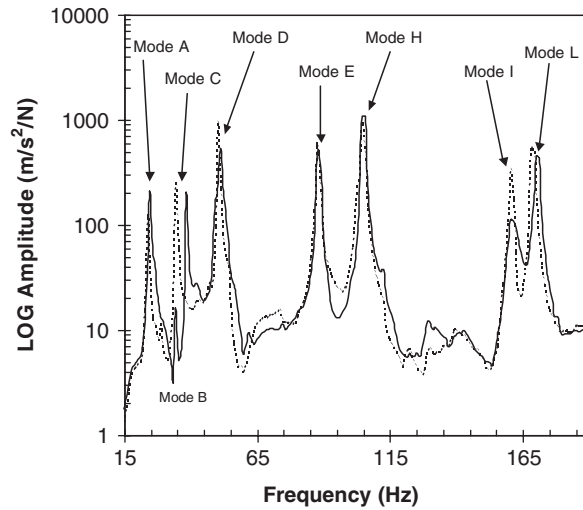


Fig. 3. Sum of all the experimental FRFs of the plate with attached mass. —, Case 3; ----, variant of Case 3 (almost same mass and rotary inertia of Case 3 but located on one side only).

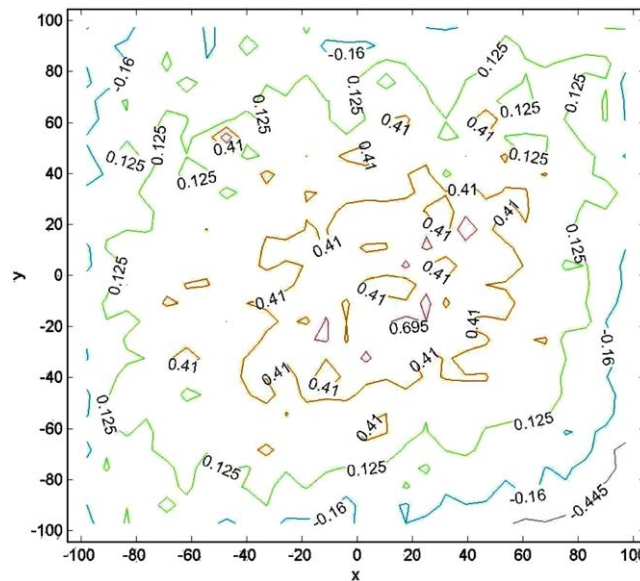


Fig. 4. Contour plot indicating measured geometric imperfection as deviation from flat surface. Deviations are in millimeters.

concentrated masses. It must also be observed that mass load gives initial deflection to the plate (in our case reducing the initial imperfection), which is not taken into account in the present numerical calculations.

4. Conclusions

Numerical results are successfully compared to experiments performed on a stainless-steel plate with an attached mass of different translational and rotary inertia. In particular, it is shown that a small mass placed on the diagonal of a square thin plate is enough to transform the shape of modes ($m = 1, n = 2$) and ($m = 2, n = 1$) into diagonal modes, i.e. modes with diagonal nodal lines. Rotary inertia of concentrated masses reduces significantly the natural frequencies. Moreover, additional modes due to the presence of large rotary

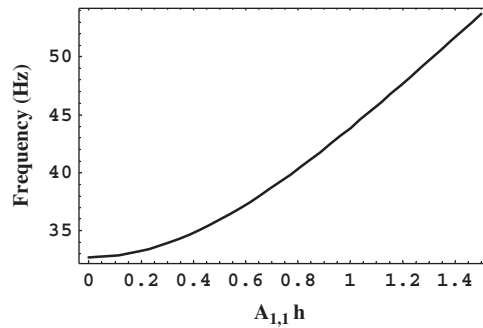


Fig. 5. Natural frequency of the fundamental mode of the plate without masses versus the amplitude of imperfection $A_{1,1}$ normalized with respect to h .

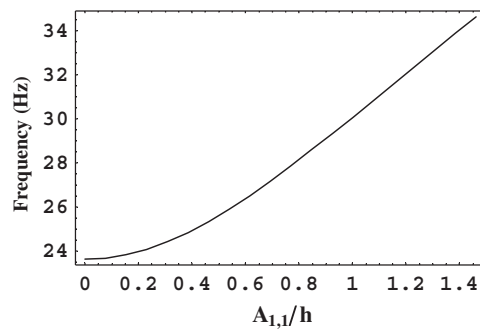


Fig. 6. Natural frequency of the fundamental mode of the plate versus the amplitude of imperfection $A_{1,1}$ normalized with respect to h ; Case 3.

inertia of concentrated masses arise, which do not appear if rotary inertia is neglected. Symmetric and not symmetric distribution of masses with respect to the plane $z = 0$ have been experimentally tested; they give very similar behaviour, suggesting to use lumped elements to model added masses with rotary inertia in finite element models.

The plate used in the experiments has been measured and present significant geometric imperfections. This indicates that geometric imperfections can play a significant role in practical applications for thin plates.

Acknowledgements

This work was partially supported by the FIRB 2001 and COFIN 2003 Grants of the Italian Ministry for University and Research (MIUR). The support of company BPS at Pero (Milano), that provided the Polytec laser Doppler vibrometer, is acknowledged.

References

- [1] S. Gershgorin, Vibrations of plates loaded by concentrated masses, *Prikladnaya Matematika i Mekhanika* 1 (1933) 25–37 (in Russian).
- [2] A. W. Leissa, *Vibration of Plates*, NASA SP-160. Washington, DC: Government Printing Office, 1969. Now available from The Acoustical Society of America (1993). See 141–151.
- [3] W.F. Stokey, C.F. Zorowski, Normal vibrations of a uniform plate carrying any number of finite masses, *Transactions of the ASME, Journal of Applied Mechanics* 26 (1959) 210–216.
- [4] A.H. Shah, S.K. Datta, Normal vibrations of a rectangular plate with attached masses, *Transactions of the ASME, Journal of Applied Mechanics* 36 (1969) 130–132.

- [5] J.W. Nicholson, L.A. Bergman, Vibration of thick plates carrying concentrated masses, *Journal of Sound and Vibration* 103 (1985) 357–369.
- [6] R.K. Singal, D.J. Gorman, A general analytical solution for free vibration of rectangular plates resting on fixed supports and with attached masses, *Transactions of the ASME, Journal of Electronic Packaging* 114 (1992) 239–245.
- [7] P.A.A. Laura, C.P. Filipich, V.H. Cortinez, Vibrations of beams and plates carrying concentrated masses, *Journal of Sound and Vibration* 117 (1987) 459–465.
- [8] J. Awrejcewicz, V.A. Krysko, 3-D theory versus 2-D approximate theory of free orthotropic (isotropic) plate and shell vibrations—part 1: derivation of governing equations, *Journal of Sound and Vibration* 226 (1999) 807–829.
- [9] J. Awrejcewicz, V.A. Krysko, 3-D theory versus 2-D approximate theory of free orthotropic (isotropic) plate and shell vibrations—part 2: numerical algorithms and analysis, *Journal of Sound and Vibration* 226 (1999) 831–871.
- [10] K.H. Low, G.B. Chai, T.M. Lim, S.C. Sue, Comparisons of experimental and theoretical frequencies for rectangular plates with various boundary conditions and added masses, *International Journal of Mechanical Sciences* 40 (1998) 1119–1131.
- [11] M. Amabili, R. Garziera, Vibrations of circular cylindrical shells with nonuniform constraints, elastic bed and added mass—part I: empty and fluid-filled shells, *Journal of Fluids and Structures* 14 (2000) 669–690.
- [12] W. Ostachowicz, M. Krawczuk, M. Cartmell, The location of a concentrated mass on rectangular plates from measurement of natural vibrations, *Computers and Structures* 80 (2002) 1419–1428.
- [13] M. Amabili, Nonlinear vibrations of rectangular plates with different boundary conditions: theory and experiments, *Computers and Structures* 82 (2004) 2587–2605.